Spectral Differences Between Two Acoustic Imaging Methods for the *in-situ* Evaluation of Surface-Breaking Cracks in Asphalt

M Iodice, J M Muggleton and E Rustighi

Institute of Sound and Vibration Research, University of Southampton; Southampton, United Kingdom

E_mail: michele.iodice@gmail.com

Tel. No.: +44(0)7767715748

Abstract: The assessment of the location and the extension of cracks in roads is important for determining the potential level of deterioration in the road overall and in the infrastructure buried beneath it. Damage in a pavement structure is usually initiated in the tarmac layers, making Rayleigh waves ideally suited for the detection of shallow surface defects. Assessment of crack in roads is usually performed assuming constant velocity and non-dispersive behaviour of the material tested, limiting this approach to the very shallow layer of the road. In this work, differences between the spectral images obtained with the Multichannel Analysis of Surface Waves (MASW) and the Multiple Impact of Surface Waves (MISW) are exploited for the first time to detect, locate and evaluate

surface-breaking cracks in dispersive material, i.e. roads. The road is holistically treated as a dispersive medium, supporting a paradigm-shifting approach to *in-situ* crack evaluation. It is shown that surface-breaking cracks influence the content of the spectral images obtained with these two acoustic imaging techniques. Their differences are used for the first time for the *in-situ* evaluation of the presence, the location and, in some cases, the extension of vertical cracks in roads. The study is conducted through numerical simulations, alongside experimental investigations. The paper describes two cases for which the cracking is internal and then external to the deployment of sensors. The method proposed in this paper proved to be successful for the *in-situ* evaluation of cracks in asphalt, tackling the heterogeneities and dispersive behaviour of the material tested.

Keywords: cracks, asphalt, MASW, R-wave, *f-k*, FEM.

1. Introduction

Paved roads provide a smooth and regular surface for vehicles to move along easily and safely. The structure of the paved road usually consists of a multi-layered system of bitumen-bound and unbound materials disposed on top of each other, constituting in fact a highly dispersive system. The main purpose of the layers is to distribute traffic loads from the vehicles to the underlying natural soil. Routinely investigation of the structural integrity of the road network is of primary importance [1]. The budget needed

for engineering maintenance of highways in England (excluding London) in 2017 was of £3.05 billion. This number is expected to grow over the next few years in order to address a backlog in the maintenance required and increasing deterioration of the road network [2].

One of the ways in which damage in a pavement road structure manifests itself is in cracking, which is most commonly initiated in the asphalt layers. This makes Rayleigh wave (R-wave) ideally suited for the detection of shallow surface defects through non-destructive techniques (NDTs). The proper assessment of the location and of the extension of such discontinuities is crucial for the determination of the level of deterioration of an infrastructure and for decisions regarding maintenance, strengthening and rebuilding of existing infrastructures. In fact, surface-breaking cracks in concrete and asphalt are symptoms of incipient failure of the structures [3]. For the aforementioned reasons, R-wave has been exploited by many to monitor asphalt and concrete deterioration [1], [3]–[7].

It has been well established that a drop of about 30% in the initial (i.e. at the beginning of the infrastructure's service life) value of the stiffness modulus of asphalt is a signal of incipient failure, or in other words, the beginning of the phenomenon of fractures [8]. Although it seems possible to measure the residual life of an infrastructure by monitoring the stiffness over time, there are significant challenges still to be addressed. For example, a reference value of the stiffness for every different asphalt mixture is required. Adding to the problem complexity is the fact that the influences of temperature and self-repairing mechanisms ongoing in an asphalt pavement during its life are yet to be understood, and that seismic methods for monitoring asphalt

deterioration should be able to cope with the inhomogeneity, anisotropy and dispersive nature of the road system.

The majority of the current state-of-the-art in evaluation of cracks in asphalt with acoustic methods are based on the detection of very shallow, top-down cracks in homogeneous, non-dispersive, monochromatic, single-mode, single-layered slabs or specimens, and on the assumption of constant velocity at ultrasonic frequencies [9]–[11]. Current methods deliberately ignore the complex, dispersive, inhomogeneous, multi-mode, layered features of the road system overall and especially of the inner road layers, and do not support *in-situ* applications. To the authors' knowledge, there are no routinely methods for the *in-sit*u detection and assessment or vertical cracks in roads.

Nonetheless, a thorough review of the common approaches to crack detection and evaluation in non-dispersive materials is essential. Non-destructive techniques to characterize and estimate the depth of surface-breaking cracks in non-dispersive materials, like concrete and metals, can be classified in two major categories: time-of-flight based approaches (in the time domain) and frequency based approaches (in the frequency domain) [12]. Time-of-flight methods are based on the estimation of the time required for a longitudinal wave to travel from the location it was originated, to the opposite side of the crack, travelling across the tip of the surface-breaking crack [12]. These methods are explored by many authors as a tool for crack interrogation[13], [14], and they often proved to be accurate when applied to real structures [3], [12].

On the other hand, frequency based methods rely on the analysis of data in the frequency domain after some types of transformation (e.g. Fourier, Wavelet, frequency-wavenumber). The vertical crack has a resonance-type feature which occurs periodically

at certain frequencies and has found to be associated with the depths of the cracks [14]–[16]. Moreover the edges of surface defects like cracks act like a source that excites surface waves which propagate along the crack surface [13], [16]. The finite depth of the crack blocks shorter-wavelengths, allowing only the longer wavelengths to proceed and hence it acts as a low-pass filter. In general, cracks are likely to generate reflections and to change both the time history and the frequency content (the spectral response) of a seismic signal at the surface [17].

Detection of vertical cracking with frequency methods is often based on the study of the scattered R-wave from the boundaries of the crack, even though reflections from the surfaces of the crack have weak energy and limited frequency range, making this process difficult to implement [17]. Particularly, the resonant effects of the scattering waves [18] or leaky Rayleigh waves [14] in the ultrasonic range of frequencies are exploited to extract the information about the depth and the length of a surface crack, with ambiguous results. Wave transmission and attenuation measurements and the spectral ratio of the transmitted wave on the incident wave are also exploited by various authors for detection and sizing of surface discontinuities [3], [19], [20].

Numerical and experimental investigation support the use of frequency based methods for crack and voids detection [17], [21]. Numerical approaches to surface-breaking discontinuity detection show that the dispersion curve, and hence the wavefield, changes if the signal travels across a vertical discontinuity, which can be a crack or a slot [21]. An investigation on a homogeneous Plexiglas sheet suggested the use of an array of sensors to compute the power spectral density for the location of the cracking, and the use of frequency-wavenumber spectral images obtained from the same array of sensors

for the assessment of the crack depth [19]. Although the power spectral density showed to be sensitive to the crack location, the assessment of depth proved to be inaccurate. Other numerical studies suggest a time-frequency analysis of the response for anomaly detection in layered media based on the wavelet transform [17]. Time differences between energy maxima and the range of frequencies of different energy levels in the time-frequency spectral image could lead to the estimation of the approximate location and size of the defects.

Despite frequency based and time-of-flight based methods showed to be often successful, at various degrees, in estimating the depth of surface cracks in non-dispersive materials, the practical and reliable, *in-situ* evaluation of cracks in asphalt needs to take into account the heterogeneous nature of the materials tested and its dispersive behaviour. This inevitably makes these methods dependent on the velocity of the material at different depths and frequencies. Dispersive behaviour is often deliberately ignored or underestimated. Simplistic approaches based on the assumption of non-dispersion and of constant phase velocity lead to troublesome crack detection strategies [22].

In this paper, the potential of the MASW and the MISW method to be synergistically used for the *in-situ* evaluation of surface-breaking cracks in dispersive media, i.e. roads, is investigated for the first time. In fact, surface-breaking cracks influence the content of the spectral image obtained with the two methods in different ways. The proposed method leverages the differences in the spectral images obtained with MASW and with MISW to extract meaningful information about location and size of the surface-breaking crack. For the first time, the assumption of consistent phase velocity and of non-

dispersive behaviour, is lifted. Only top-down cracks are considered in this study, i.e. cracks initiated from the surface. Since they are visible, it is easier to perform a preliminary study for validation. Two scenarios are investigated in the forthcoming investigations, for which the crack is external and across the deployed array of geophones.

The proposed method proved to be successful for the detection, the location and, in some cases, the assessment of the depth of surface-breaking cracks both numerically and experimentally, tackling the dispersive and heterogeneous nature of asphalt. The method is an add-on of the two aforementioned NDTs, which are already commonly utilized for the *in-situ* estimation of the structural properties (thickness and stiffness) of the different layers of a road system, and hence it could be easily adopted in real practice as no additional training is required.

2. Description of proposed seismic imaging methods

The most common methods for imaging of roads using R-wave are the Multichannel Analysis of Surface Waves (MASW) and the Multiple Impact of Surface Waves (MISW). They both share two basic steps for the calculation of the layers' stiffness: the measure of an experimental dispersion curve and the estimation of a layer model by matching the measured dispersion curve with a theoretical dispersion curve (inversion) [23]. Multichannel Analysis of Surface Waves (MASW) is the most utilized seismic imaging method for road surveys, due to its advantages in dispersion measurement of irregular profiles [24], [25]. The set-up configuration consists of a source of seismic energy and multiple receivers (typically 24, but also up to 48 or more) placed on the ground surface

with an equal spacing along a survey line (Figure 1) [26], [27]. The source offset and the spacing D between receivers are chosen according to the maximum frequency to sample; the length according to the maximum depth of the survey and to the resolution to be achieved. The vertical ground vibration response is recorded simultaneously by all the receivers. MASW typically uses continuous sources like shakers or impulsive sources like sledgehammers [28], [29], exciting frequencies typically up to 10kHz [1]. In MASW the experimental data is typically transformed from the offset-time domain (*x*-*t*) to the frequency-wavenumber (*f*-*k*) domain using a 2-D Fourier transform. This allows different wave-types and higher order Rayleigh modes (typical of not-normally dispersive media) to be distinguishable in the spectral image [28], [30], [31] The measured dispersion curve obtained with MASW is then inverted to match that of a theoretical model with known structural properties.

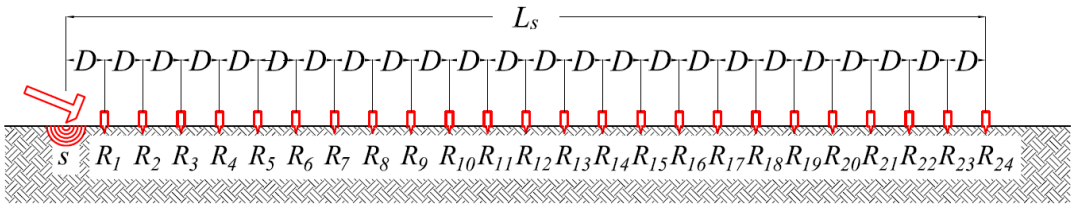

Figure 1. Typical MASW set-up configuration in the case of an isotropic medium with absence of discontinuity, where *R* refers to a geophone, *s* refers to a source of seismic energy, *D* is the receiver spacing, L_s is the length of the deployment of sensors.

Sometimes a true multichannel survey can be cumbersome, requiring many bulky receivers deployed simultaneously in a small area. Multiple Impact Surface Waves

(MISW) is an alternative to the common MASW technique, which takes advantages of homogeneity, in order to obtain a multichannel record in an easier and faster way (see Figure 2). MISW employs a limited number of sensors (possibly only one as in the multichannel simulation with one receiver (MSOR)), compared to MASW [1], [27], [32]. The source is consecutively moved by the same distance along the survey line whilst sensors are not moved: eventually, a simulated multichannel record is constructed by compiling the subsequent seismic traces and the data transformed in the *f-k* domain via a 2-D Fourier transform. MISW becomes advantageous for the assessment of roadways, since the coupling between asphalt surface and sensors can be difficult to achieve.

If MISW and MASW are used on the same portion of road, the same spectral image is obtained, so long as the road system is homogeneous, i.e. the mechanical properties do not change transversally and longitudinal and transversal discontinuities are absent.

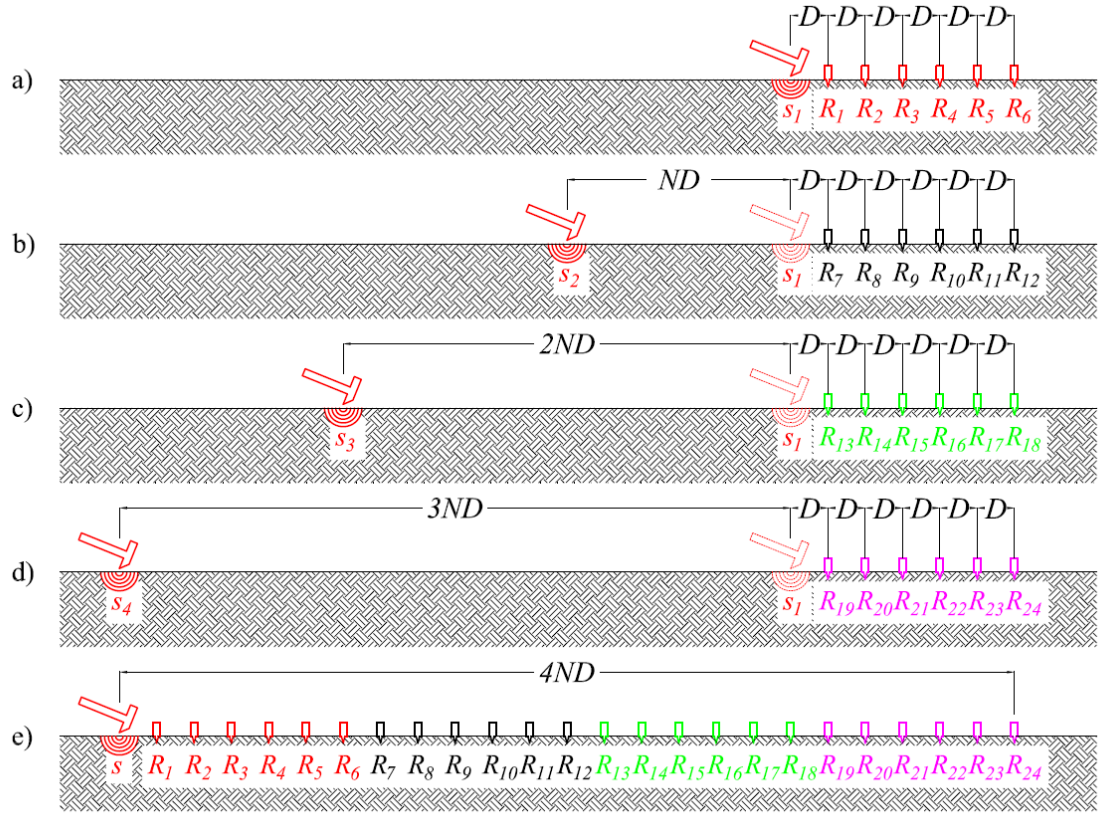

Figure 2. Typical MISW set-up configuration in the case of an isotropic medium with absence of discontinuity, where *R* refers to a geophone, *s* refers to a source, *D* is the receiver spacing, *N* is the number of receivers, *ND* is the length of the deployment of sensors. The source is consecutively moved apart by the same distance from the first, second and third measurement (a, b, c) to the last (d) leading to an equivalent multichannel configuration (e). If mechanical properties do not change transversally, MISW and MASW surveys lead to the same results.

In the presence of a crack external or internal to the deployment of geophones, the MISW technique adds a fictitious periodicity to the system, since the presence of the discontinuity is artificially repeated every time the source is moved apart (see Figure 3 and Figure 4). The crack in the figures appears as normal to the surface for the sake of

illustration, but the method applies also to inclined cracks. The advantages of the combinatory use of the two aforementioned imaging techniques for the detection of cracks in asphalt are illustrated through experimental and numerical investigations in the next sections.

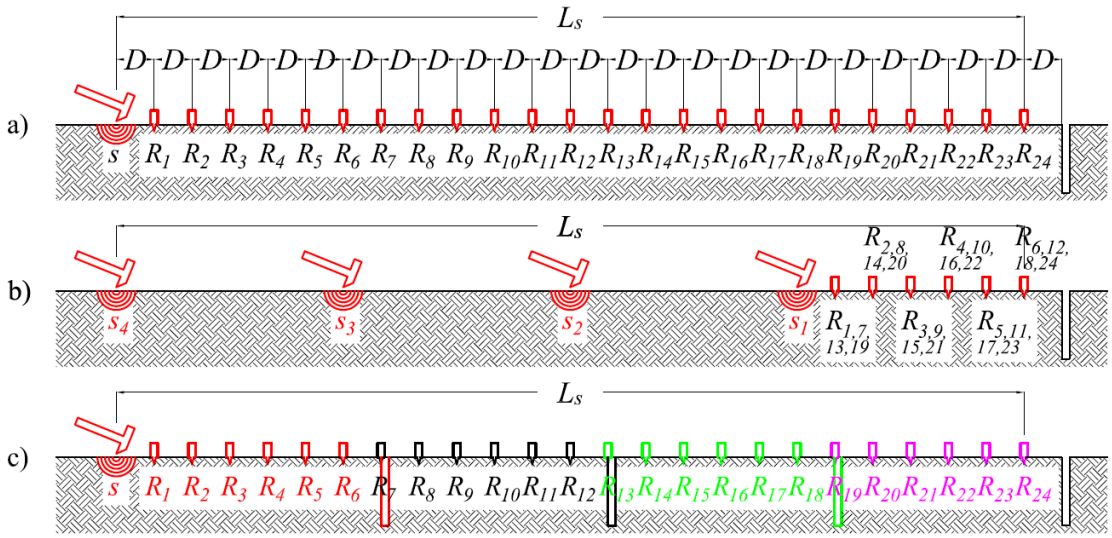

Figure 3. MASW set-up configuration (a), MISW set-up configuration (b) and its equivalent multichannel configuration (c) adopted for the forthcoming numerical and experimental investigation in the case of a discontinuity located outside the deployment of sensors.

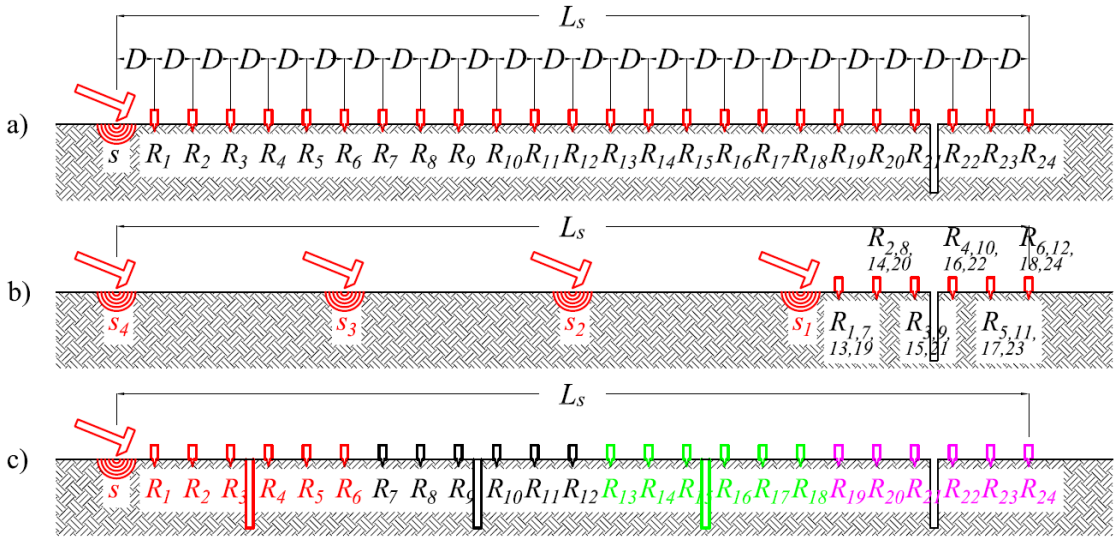

Figure 4. MASW set-up configuration (a), MISW set-up configuration (b) and equivalent multichannel configuration (c) adopted for the forthcoming numerical and experimental investigation in the case of a discontinuity located within the deployment of sensors.

3. Numerical model

A two-dimensional finite element model of the ground is assembled through the Abaqus/CAE software to study the wave propagation in half-spaces and layered systems.

3.1. Features of the model

The analysed profile consists of a top layer over a half-space simulating a road with irregular stratification (i.e. the velocity decreases with depth), with a weak (damaged) asphalt layer overlaying a base/foundation layer.

The model used in this paper is semi-elliptical in shape, with semi-major axis of 10 m and semi-minor axis of 7.5 m. Each layer is considered to be elastic and isotropic. In this paper both finite and infinite elements are used in combination for the ground model:

a 3-node bilinear triangle (CPE3) and a 4-node bilinear quadrilater (CINPE4). The biggest issue with numerical simulation of wave propagation in multi-layered systems is to avoid, or at least minimize, the effects of reflection of the wavefronts from the boundaries, and hence to properly model P-wave, S-wave and R-wave [33]. To address this specific issue, in the work presented here, infinite elements are applied to the boundaries of the model.

Following the work of Zerwer [34], since we only have interest in surface wave measurements, the mesh element size progressively increases in the downward vertical direction. This choice is motivated by two factors. Firstly, the higher frequencies travel at the shallow surface, where a certain mesh size is required. Lower frequencies travel at lower depths with bigger wavelength, so a bigger mesh size is acceptable. Secondly, R-wave decays exponentially with depth, i.e. most of the R-wave energy is located within the depth of one wavelength. The use of infinite elements enables the model to be much smaller in size, since we can ignore the reflection from the boundaries, especially in the case of high stiffness values and hence fast shear wave velocities. The mesh elements are smaller near the surface, where Rayleigh wave propagates, with an element size $l_{\max}$ equal to 0.05 m.

3.2. Model discretization, limitations and attenuation

With finite elements methods, two discretization constraints should be adopted in order to achieve appropriate spatial and temporal resolution. The spatial condition assures that a sufficient number of points in space are sampled in order to recreate the wave,

or in other word that the element size $l_{\max}$ is small enough (it is the analogue of the Nyquist's criterion in the time domain) [34], [35]:

$$f_{\max} \leq \frac{V_S}{2 \cdot l_{\max}} \tag{1}$$

where V_S is the shear velocity and $f_{\max}$ is the maximum frequency.

The temporal constraint must be set after the spatial one, to ensure that the wave front does not travel faster than the time step Δt. This is achieved using the Courant-Friedrichs-Lewy condition [34], [36], [37], here rearranged for two-dimensional problems:

$$\Delta t_{\max} \leq \frac{1}{V_P \sqrt{\frac{1}{l_{\max}^2}}} \tag{2}$$

where V_P is the compressional wave velocity.

Damping in numerical simulations is usually expressed as Rayleigh damping in terms of the mass damping α and the stiffness damping β, as follows [18]–[21]:

$$\xi = \frac{1}{2\omega}\alpha + \frac{\omega}{2}\beta \tag{3}$$

where ξ is the damping ratio and ω is the angular frequency of excitation.

It can be noticed that the damping ratio varies with the frequency of excitation. Stiffness damping, β, varies according to each simulation, whereas mass damping, α, is set equal to zero, following the work of Zerwer [21] and of Jou-Yi Shih [39], in the attempt to avoid high damping at low frequencies and the presence of numerical parasitic modes.

The parameters of the model are given in Table 1. Mechanical parameters, density and damping ratios have been chosen to represent a road pavement system, with a stiff layer

over a softer layer. They are chosen to be representative of typical values of soils and asphalts, and are similar to those used in [17], [40]–[42].

The discontinuity is a rectangular, vertical, empty notch 0.18 m deep and 0.01 m wide. A big, wide, empty crack serves the purpose of validating and proving the concept of the proposed method. All the simulations are carried out with a sampling frequency of 50 kHz. The load used in the simulation consists of a short Hanning window ranging from 0 sec to 0.0004 sec, capable of properly exciting frequency up to a value of 3 kHz. This impulsive load is used in an attempt to simulate the impulsive impact of a mallet with the ground.

Table 1. Parameters of the FEM model.

Poisson ratio, ν	1/3
Mass density, ρ	$2000\ \mathrm{kg \cdot m^{-3}}$
Minimum wavelength	$0.10\ \mathrm{m}$
Semi-major axis	$10\ \mathrm{m}$
Semi-minor axis	$7.5\ \mathrm{m}$
Time step, Δt	$2 \cdot 10^{-5}\mathrm{sec}$
Maximum frequency, $f_{\max}$	4050 Hz
Duration of the simulation T	$0.10\ \mathrm{sec}$
Thickness upper layer, h	$0.20\ \mathrm{m}$
Thickness half-space	∞
Mass damping, α	0
Stiffness damping upper layer, β_1	$0.01/(200 \cdot 2\pi)$
Stiffness damping half-space, β_2	$0.025/(200 \cdot 2\pi)$
Young's Modulus upper layer, E_1	2000 MPa
Young's Modulus half-space, E_2	1000 MPa
R-wave velocity upper layer	$571\mathrm{m \cdot s^{-1}}$

R-wave velocity half-space	$405\mathrm{m}\cdot\mathrm{s}^{-1}$

3.3. Frequency-Wavenumber transformation

The *f-k* transformation is a two-dimensional Fourier Transform which converts the vertical space-time domain representation $u(x,t)$ of a seismic event into the frequency-wavenumber representation $U(f,k)$: the time information is transformed into frequency components and the spatial information is transformed into wavenumber components. The peaks of the $U(f,k)$ spectrum are associated with the energy maxima and hence to the vibrational modes of propagation. The transformation is a well-established method and its properties are reported in many works [30], [43]–[46].

The resolution of the image in the *f-k* domain is inversely proportional to the length T of the signal in time and to the length L_s of the sensor line in space (trivially, the number of geophones). Spacing between geophones dictates the maximum wavenumber. The resolution is a key factor in separating the different modal contributions: often a peak in the *f-k* domain is not associated with a single mode, but is rather a superposition of several different modes. This can then lead to erroneous interpretation of the results. The *f-k* transform can discriminate between direct positive going waves (characterized by positive wavenumbers) and negative going waves (characterized by negative wavenumbers) [34].

The shear wave velocity profile (shear wave velocity and R-wave velocity are linearly correlated [47]) is usually obtained through a numerical inversion of the experimental dispersion curve obtained from the energy maxima of the spectral image, trying to match the experimental dispersion curve with that coming from an analytical or a numerical model.

Figure 5 shows the *f-k* spectrum of the undamaged case obtained with the numerical model described in Table 1, the MASW set-up configuration of Figure 1 and the MISW set-up configuration of Figure 2. The spectral images obtained with the two methods perfectly coincide, if we are in the situation of absence of discontinuities and heterogeneities. The purple bands correspond to the direct Rayleigh wave modes of propagation. The energy at low frequencies is usually higher than the energy associated to the higher frequencies, due to intrinsic attenuation.

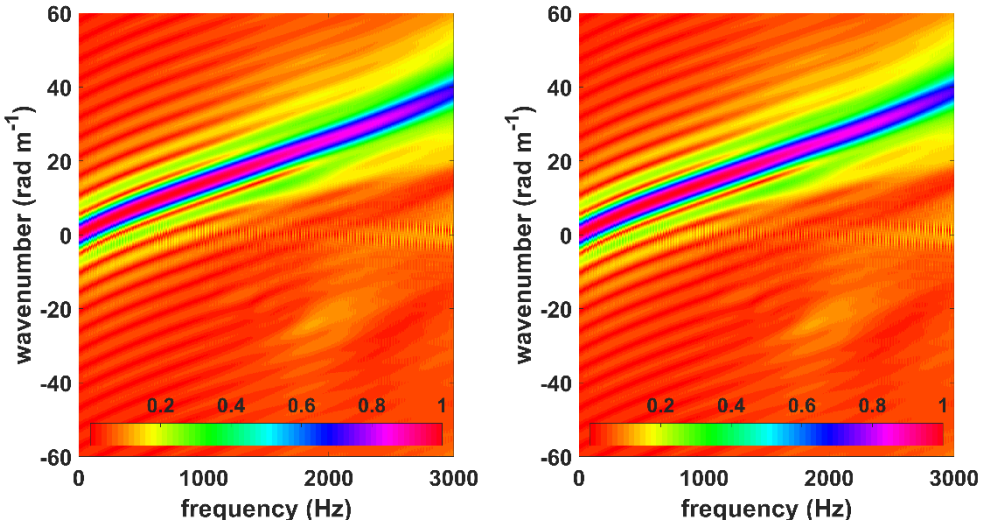

Figure 5: The *f-k* spectrum of the undamaged case obtained with the MASW set-up (a) and with the MISW set-up (b).

4. Numerical investigation

A total of four different numerical simulations were run with the MASW and the MISW techniques, with an array of 24 sensors as in the configurations displayed in Figure 3 and Figure 4. They aimed at showing the different effects of a discontinuity on the *f-k* spectral images obtained from MASW and MISW.

4.1. Numerical simulation with a crack external to the deployment of sensors

The first two simulations aim at comparing the MASW and MISW techniques for detection of a crack situated outside the deployment of sensors with the spacing D equal to 0.05 m.

In the presence of a vertical discontinuity outside the deployment of sensors, the *f-k* spectrum obtained with a MASW technique shows energy maxima corresponding to the direct Rayleigh modes of propagation (Figure 6(a)). These maxima carry the largest amount of energy and are then associated with the purple band in the spectrum. One can also notice the presence of the negative going Rayleigh wave reflected by the boundaries of the anomaly, characterized by negative wavenumbers and highlighted by the white arrow in Figure 6(a). The energy associated to the reflected negative going wave is very weak and the reflection shows limited duration with the higher frequencies decaying very fast.

The *f-k* spectrum obtained with a MISW technique (Figure 6(b)) shows energy maxima corresponding to the direct Rayleigh modes of propagation, as with the MASW technique, associated with the purple band in the spectrum. The frequency bandwidth of the direct Rayleigh modes is comparable with the band obtained with MISW. One can also notice the presence of additional energy maxima in the negative wavenumbers region. They are parallel to the direct Rayleigh wave and they are produced by the reflections from the faces of the vertical discontinuity. These energy maxima are distributed in a diagonal pattern such as to follow the slope of the reflected negative going wave (negative wavenumbers). Moving the source and keeping the sensors in a fixed position adds a periodicity in the system (see Figure 3 and Figure 4) and in the time-

space representation, resulting in fictitious energy maxima also in the frequency-wavenumber domain. These maxima are highlighted by arrows in Figure 6(b) and they are spaced by an offset Δp proportional to the length ND of MISW's deployment of sensor, as follows:

$$\Delta p = \frac{2\pi}{\mathrm{ND}} (\mathrm{rad \cdot m^{-1}}) \tag{4}$$

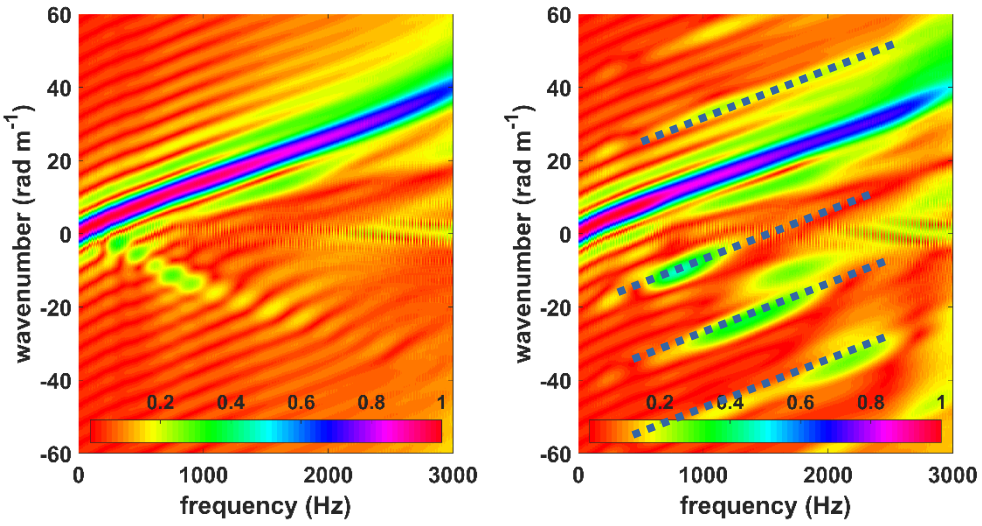

Figure 6. *F-k* spectrum obtained with MASW (a) and with MISW technique (b) from FEM simulations with a crack external to the array of sensors. The white arrows highlight energy maxima produced by reflections from the faces of the vertical discontinuity. The black dotted lines highlight the offset Δp.

In this simulation the offset Δp is equal to 20.94 rad m^{-1}, as N is equal to 6 and D is equal to 0.05 m. It does not depend on the crack location or size, but it is solely dependent on the fictitious periodicity added by MISW (section 2). It is highlighted by dotted lines in Figure 6. When MISW is adopted, the reflections from the boundaries of the anomaly

are enhanced, hence more visible, as can be noticed from a comparison between the two *f-k* spectra. These findings confirm that a vertical discontinuity can be detected by observing the differences between the spectral images obtained with MISW and MASW. Since the frequency bandwidth of the direct R-wave in the two spectral images is comparable and no cut-off frequencies are visible, the crack is estimated to be outside the deployment of sensors.

4.2. Numerical simulation with a crack within the deployment of sensors

The following simulations aim at comparing the MASW and the MISW techniques in the case of a crack situated within the deployment of sensors with the spacing D equal to 0.10 m. As in the previous simulations, the *f-k* spectrum obtained with a MASW technique (Figure 7(a)) shows energy maxima corresponding to the direct Rayleigh modes of propagation, corresponding to the purple bands. Very weak reflected energy is present and barely visible in the form of energy maxima at negative wavenumbers (white arrows). By looking at the spectrum of Figure 7(a), it is impossible to infer the presence of some sort of discontinuity (due to the very weak presence of reflected energy in the negative wavenumber).

The *f-k* spectrum obtained with the MISW technique (Figure 7(b)) also shows energy maxima parallel to the direct Rayleigh wave. As discussed in section 3.1, these are an indicator of the presence of the vertical discontinuity. These maxima are spaced by an offset Δp, following equation (4), and are highlighted by white arrows in Figure 7(b). In this simulation the offset Δp is equal to 10.50 rad m^{-1}, as N is equal to 6 and D is equal to 0.10 m. It is highlighted by dotted lines. Energy associated with reflection is much higher than the MASW case, helping with the detection of the vertical notch.

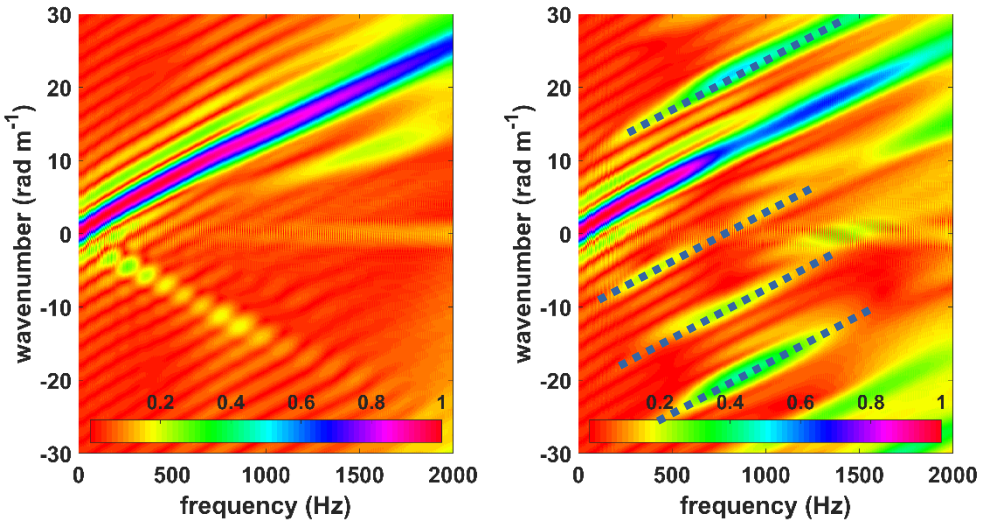

Figure 7. *F-k* spectrum obtained with MASW (a) and with MISW technique (b) from FEM simulations with a crack internal to the array of sensors. The white arrows highlight energy maxima produced by reflections from the faces of the vertical discontinuity. The black arrow highlights the frequency of cut-off due to the presence of the crack. The black dotted lines highlight the offset Δp.

Moreover, the energy associated with the direct Rayleigh wave, although noticeable up to a frequency of approximately 2 kHz, becomes abruptly weaker above 1 kHz. The latter can be identified as a cut-off frequency and it is highlighted in the spectrum by a black arrow. In fact, the discontinuity acts as a low-pass filter, reducing the energy flowing into frequencies higher than the frequency of cut-off. This phenomenon indicates that the discontinuity is located across MISW's deployment of sensors of Figure 4(a), or in its proximity. Assuming the R-wave velocity equal to 500 m s^{-1} at the frequency of cut-off (from Figure 7), and bearing in mind that the representative depth of each frequency component of R-wave is assumed equal to one third of the wavelength, the depth of the

notch can be evaluated to be equal to 0.17 m. Compared to the real depth of the crack, the estimation accomplished from the frequency of cut-off is very accurate.

As for the previous case (section 4.1), the vertical discontinuity can be detected by observing the differences between the spectral images obtained from MISW and from MASW. Particularly, the energy associated to the direct R-wave spreads across different frequency bandwidths. The frequency of cut-off in the MISW's spectrum suggests that the crack is located across MISW's array, or in its proximity. The depth of the crack can be roughly estimated from the value of the frequency of cut-off.

5. Experimental investigation results & discussion

This experimental investigation consisted of two separate studies: in the first study the two different seismic technologies were compared for the detection of a real discontinuity external to the array of sensors, while in the second they were adopted in a real case of a crack within the array of sensors. Two separated sites were tested for the aforementioned cases. The data was acquired using a ProSig P8020 data acquisition unit and a laptop. In the experimental investigation all the tests were repeated and recorded 5 times with a sample frequency of 8 kHz and duration T of 1 sec, under the same input conditions, and then averaged in the frequency domain. For the purposes of this work, tri-axial geophones SM-24 from ION Sensor Nederland with a cut-off frequency of approximately 1 kHz were used. Big, wide, visible cracks and discontinuities were chosen solely as a proof of concept of the proposed method and for being of known location.

The MASW experimental set-up consisted of an array of 24 geophones with a spacing D equal to 0.10 m, covering an overall length L_s of 2.40 m. The MISW experimental set-up

consisted of an array of 6 geophones with the spacing D equal to 0.10 m, covering a length L_s of 0.60 m.

In the first investigation, the vertical discontinuity was represented by the transversal edge of the asphalt wearing course of the road, as shown in Figure 8(a). The source consisted of a light metallic mallet striking on a circular plate of 0.15 m diameter, merely laid down the surface. The auto-spectrum computed from the signal of an accelerometer attached to the surface of the plate (shown in [48]) revealed that the energy was evenly distributed over a range of frequencies varying from 10 Hz to 4 kHz.

For the second investigation, a 0.01 m wide vertical cracking visible from the surface was located across the geophone array. For this investigation, the mallet was used directly onto the surface, with a similar frequency response to the first experiment [48].

(a) (b)

Figure 8. The two discontinuities investigated experimentally. Outside the geophone array in (a) and within the array in (b).

5.1. Experimental investigation with a crack external to the deployment of sensors

The *f-k* spectrum obtained with the MASW technique is shown in Figure 9(a), whilst the spectrum obtained with the MISW technique is shown in Figure 9(b). In both spectra the largest amount of energy corresponds to the direct Rayleigh wave propagation modes, associated with the purple bands. The behaviour of the propagation modes of the Rayleigh wave follows that of layered irregular systems, i.e. system where the shear velocity decreases with depth. A mode jump is noticeable at a frequency of approximately 200 Hz. With the MASW technique only weak reflected energy is visible (white arrow in Figure 9(a)). Nevertheless, from this plot alone is not possible to establish the presence of a discontinuity.

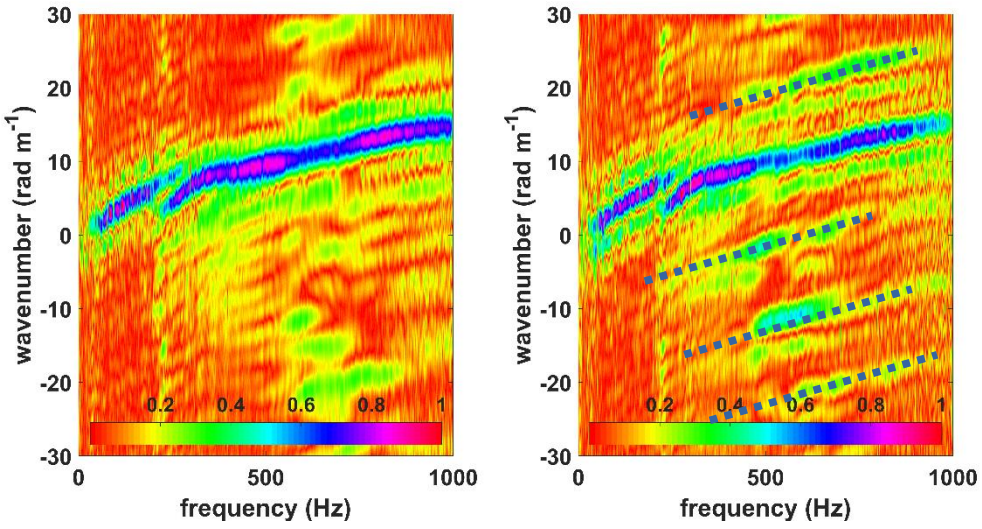

Figure 9. *F-k* spectrum obtained with MASW (a) and with MISW technique (b) from the experimental investigation with a crack external to the array of sensors. White arrows highlight energy maxima produced by reflections from the faces of the vertical discontinuity. The black dotted lines highlight the offset Δp.

Instead, by comparing the spectral images obtained with MASW and with MISW it is possible to observe substantial differences. In fact, additional energy maxima parallel to the ones associated with the direct Rayleigh wave are noticeable in the MISW's spectrum, which are an indicator of the presence of the vertical discontinuity. The maxima are spaced by an offset Δp, following equation (4), and are highlighted by white arrows in Figure 9(b). This behaviour is expected and it follows that of the numerical simulation (section 4.1). In this case the offset Δp is equal to 10.50 rad m^{-1} and it is highlighted by dotted lines.

5.2. Experimental investigation with a crack within the deployment of sensors

A second experimental investigation was executed in the case of a surface-breaking crack situated within the deployment of sensors. The *f-k* spectrum obtained with the MASW technique is shown in Figure 10(a), whilst the spectrum obtained with the MISW technique is shown in Figure 10(b).

The two spectral images display energy maxima corresponding to the direct Rayleigh modes of propagation, associated with the purple bands. The general trend of the dispersion curve follows that of irregular pavement system, where the dispersion curve breaks up into small branches of dispersion curves [49]. MASW's spectral image contains no information about the presence of vertical discontinuities. When MISW is used (Figure 10 (b)), one can notice the presence of additional energy maxima parallel to the direct Rayleigh wave modes of propagation, which are an indicator of the presence of a vertical crack. In this case the offset Δp is equal to 10.50 rad m^{-1} and it is highlighted by dotted lines.

The two spectral images show some other substantial differences. While the energy associated with the direct Rayleigh wave is noticeable until a frequency of approximately 1 kHz for the MASW case (Figure 10(a)), it becomes abruptly weaker above 200 Hz in the MISW case. Again, this behaviour is expected and it follows that of the numerical simulation (section 4.2). The frequency of cut-off is highlighted by a black arrow in the *f-k* spectrum and is due to the presence of the crack. The vertical discontinuity allows only the passage of longer Rayleigh wavelengths, blocking the passage of the shorter ones, which are mainly reflected. Hence it acts as a low-pass filter. Assuming the R-wave velocity equal to 500 m s^{-1} at the cut-off frequency of 200 Hz (from Figure 10), and bearing in mind that the representative depth of each frequency component of R-wave is assumed equal to one third of the wavelength, the depth of the crack is evaluated to be equal to 0.83 m. Whilst it was not possible to confirm this by excavation on the test site, the results indicate a very deep crack, potentially generating from the unbound layers of the road system. Remembering the frequency range of geophones, the maximum frequency detectable in these experimental studies is approximately 1 kHz.

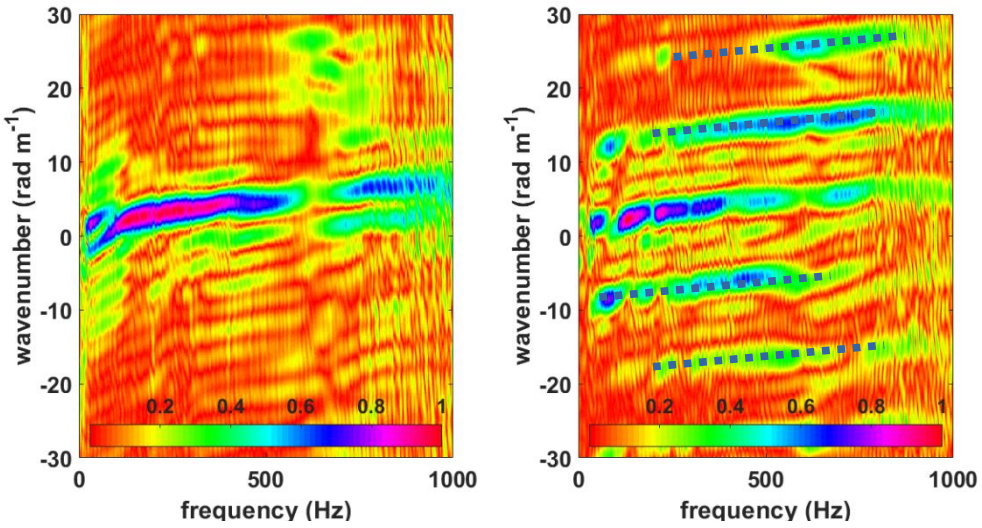

(a) (b)

Figure 10. *F-k* spectrum obtained with MASW (a) and with MISW technique (b) from the experimental investigation with a crack internal to the array of sensors. The white arrows highlight energy maxima produced by reflections from the faces of the vertical discontinuity. The black arrow highlights the frequency of cut-off due to the presence of the crack. The black dotted lines highlight the offset Δp.

5.3. Discussions

There are currently no standard methods for the *in-situ* detection and the evaluation of cracks in asphalt. Strategy to the assessment of crack detection in asphalt usually involves the assumption of constant velocity across the road system, and non-dispersive behaviour of the tested media. This work introduces a paradigm-shift in the approach to road testing, for which the assumptions on the non-dispersive behaviour are lifted, and road is approached in a holistic way and treated as a dispersive medium.

This paper proposes the synergetic application of two standard seismic imaging methods for the *in-situ* detection and interrogation of surface-breaking cracks in asphalt. The aim is to highlight the potential of extracting information about the state of the road from the differences between spectral images in the frequency-wavenumber domain. Insight into practical application for detection and interrogation of cracks in asphalt descends from the observations of the measurement shown in this paper. The proposed detection strategy would combine the MASW and the MISW measurements. Firstly, any relevant differences in the spectral images obtained with MASW and MISW would be an indicator of the presence of a vertical discontinuity. This might be located either externally or

internally to the deployment of sensors. If the frequency bandwidth of the direct R-wave in the spectral images is the same, the discontinuity is located externally. A frequency of cut-off in the MISW's spectrum is associated to a crack close to (or across) its deployment of sensors. The depth of the discontinuity can be estimated from the value of the frequency of cut-off.

The method could be scaled-up for evaluation of smaller cracks, so long as the proper spatial and frequency resolution of data is adopted (typically up to 10 kHz). Exact pinpointing of a vertical crack is not achievable, but the method would give a coarse-grained estimation of the location of the crack. Quantification of cracks is potentially possible by looking at multiple cut-off/cut-on in the spectral images, but a wider investigation with multiple cracks is needed. The method would ideally integrate the standard road survey based on the inversion of the measured dispersion curve as it effectively exploits the same set-up and data. For all the aforementioned reasons, the method could be readily adopted as a crack evaluation tool and no additional training is required. The use of air-coupled transducers, non-contact microphones or land-streamer sensor arrays could speed up the process [50].

Finally, the spectral images in the frequency-wavenumber domain can be used for the measurement of different features at the same time: the shear wave profiling, by the dispersion inversion, and the crack detection, location and assessment, by the study of the spectral images differences.

6. Conclusions

In this paper, the differences in the spectral images obtained with two non-destructive methods currently utilized for monitoring the condition of roads, the MASW and the

MISW methods, are used for identification and evaluation of cracks in asphalt layers for the first time. This work supports a paradigm-shifting approach to the *in-situ* evaluation of asphalt cracks, for which the road system is assumed to be a dispersive medium and the assumption of consistent phase velocity across the crack is lifted.

MASW and MISW do not lead to the same *f-k* spectrum if used in the presence of transversal anomalies. Any relevant differences in the spectral images obtained with the two methods are an indicator of some kind of vertical anomaly. The differences in the spectral images carry the information on the presence, location and, in same cases, the size of surface-breaking cracks of any depth across the road system.

If the crack is external to the array of sensors, the spectral differences only indicate the presence of a crack. In fact, MISW adds a fictitious periodicity in to the system, which manifests itself in the spectral image as energy leaking to maxima parallel to the main propagation mode. If the crack is internal to the array of sensors, it is also possible to identify a cut-off frequency caused by the vertical anomaly. In fact a surface-breaking crack acts like a low pass filter, allowing the passage of longer wavelengths but blocking the passage and reflecting the short ones. This phenomenon is enhanced the closer the sensors are to the discontinuity. The cut-off frequency has an inversely proportional relationship with the depth of the crack.

7. Acknowledgements

The authors gratefully acknowledge the financial support of the UK Engineering and Physical Sciences Research Council under grant EP/K021699 “Assessing the Underworld – an integrated performance model of city infrastructures”.

8. Data statement

Significant data are deposited in a secure repository in a timely manner. A description of the data (metadata) is freely available at XXX even if the data is restricted.

9. References

[1] N. Ryden, "Surface wave testing of pavements.," *J. Acoust. Soc. Am.*, vol. 125, no. 4, pp. 2603–2603, Oct. 2013.

[2] A.I.Alliance, "Annual Local Authority Road Maintenance Survey 2017," no. March, 2017.

[3] W.-J. Song, J. S. Popovics, J. C. Aldrin, and S. P. Shah, "Measurement of surface wave transmission coefficient across surface-breaking cracks and notches in concrete," *J. Acoust. Soc. Am.*, 2003.

[4] F. Hugo and N.-K. J. Lee, "Using Seismic Wave Propagation as a PMS Tool," in *4th International Conference on Managing Pavements (1998)*.

[5] M. Jurado, N. Gibson, M. Celaya, and S. Nazarian, "Evaluation of Asphalt Damage and Cracking Development with Seismic Pavement Analyzer," *Transp. Res. Rec. J. Transp. Res. Board*, vol. 2304, no. 1, pp. 47–54, 2013.

[6] D. Yuan, S. Nazarian, D. Chen, and M. McDaniel, "Use of Seismic Methods in Monitoring Pavement Deterioration During Accelerated Pavement Testing with TxMLS," *Int. Conf. Accel. Pavement Test.*, 1999.

[7] N. Gucunski and A. Maher, "Evaluation of Seismic Pavement Analyzer for Pavement Condition Monitoring," no. May, p. 117, 2002.

[8] I. N.-K. J. Lee, F. Hugo, K. H. Stokoe, "Detection and monitoring of cracks in asphalt pavement under Texas mobile load simulator testing." 1997.

[9] L. Khazanovich, R. Velasquez, and E. Nesvijski, "Evaluation of Top-Down Cracks in Asphalt Pavements by Using a Self-Calibrating Ultrasonic Technique," *Transp. Res. Rec. J. Transp. Res. Board*, vol. 1940, no. May 2016, pp. 63–68, 2007.

[10] S. Underwood, Y. R. Kim, and B. S. Underwood, "Determination of Depth of Surface Cracks in Asphalt Pavements," *Transp. Res. Rec. J. Transp. Res. Board, 143-149.*, no. November 2002, 2003.

[11] S. H. Kee and J. Zhu, "Using air-coupled sensors to measure depth of a surface-breaking crack in concrete," *AIP Conf. Proc.*, vol. 1096, pp. 1497–1504, 2009.

[12] S. W. Shin, J. Zhu, J. Min, and J. S. Popovics, "Crack depth estimation in concrete using energy transmission of surface waves," *ACI Mater. J.*, 2008.

[13] M. Hirao, H. Fukuoka, and Y. Miura, “Scattering of Rayleigh surface waves by edge cracks: Numerical simulation and experiment,” *J. Acoust. Soc. Am.*, 2005.

[14] A. Fahr and W. R. Sturrock, “Detection and Characterization of Surface Cracks Using Leaky Rayleigh Waves,” *Rev. Prog. Quant. Nondestruct. Eval. Springer*, pp. 559–568, 1985.

[15] S. Ayter and B. A. Auld, “On the Resonances of Surface Breaking Cracks,” *Proc. DARPA/AFML Rev. Prog. Quant. NDE, July1978– Sept. 1979*, no. September 1979, pp. 394–492, 1980.

[16] V. Domarkas, B. T. Khuri-Yakub, and G. S. Kino, “Length and depth resonances of surface cracks and their use for crack size estimation,” *Appl. Phys. Lett.*, 1978.

[17] N. Gucunski, P. Shokouhi, and A. Maher, “Detection and Characterization of Cavities Under the Airfield,” *NDT - Competence Saf. MATEST*, no. April, pp. 151–161, 2004.

[18] V. Domarkas, B. T. Khuri-Yakub, and G. S. Kino, “Length and depth resonances of surface cracks and their use for crack size estimation,” *Appl. Phys. Lett.*, vol. 33, no. 7, pp. 557–559, 1978.

[19] A. Zerwer, M. A. Polak, and J. C. Santamarina, “Effect of Surface Cracks on Rayleigh Wave Propagation: An Experimental Study,” *J. Struct. Eng.*, 2002.

[20] G. Hevin, O. Abraham, H. Pedersen, and M. Campillo, “Characterisation of surface cracks with Rayleigh waves: a numerical model, NDT&E Int 31 (4)(1998),” *Artic. PDF (760 K)| View Rec. …*, vol. 31, no. 4, pp. 289–297, 1998.

[21] A. Zerwer, M. A. Polak, and J. C. Santamarina, “Rayleigh wave propagation for the detection of near surface discontinuities: Finite element modeling,” *J. Nondestruct. Eval.*, 2003.

[22] D. G. Aggelis and T. Shiotani, “Surface wave dispersion in cement-based media: Inclusion size effect,” *NDT E Int.*, vol. 41, no. 5, pp. 319–325, 2008.

[23] L. V. Socco, S. Foti, and D. Boiero, “Surface-wave analysis for building near-surface velocity models — Established approaches and new perspectives,” *Geophysics*, vol. 75, no. 5, pp. 75A83-75A102, 2010.

[24] C. B. Park, J. Ivanov, R. D. Miller, J. Xia, and N. Ryden, “Seismic Investigation of Pavements by MASW Method — Geophone Approach,” 2009.

[25] C. B. Park, J. Ivanov, R. D. Miller, J. Xia, and N. Ryden, “Multichannel analysis of surface waves (MASW) for pavement-feasibility test,” *Proc. 5th SEGJ Int. Symp.*, pp. 25–30, 2001.

[26] S. Nazarian, “Shear Wave Velocity Profiling with Surface Wave Methods,” in *Geotechnical Engineering State of Art and Practice: Keynote Lectures from GeoCongress 2012, pp.221-240,* 2012.

[27] N. Ryden, C. B. Park, P. Ulriksen, and R. D. Miller, “Multimodal Approach to Seismic Pavement Testing,” *J. Geotech. Geoenvironmental Eng.*, vol. 130, no. 6, pp. 636–645, 2004.

[28] C. B. Park, R. D. Miller, and J. Xia, “Multichannel analysis of surface waves,” *Geophysics*, vol. 64, no. 3, pp. 800–808, 2002.

[29] C. Park, R. Miller, J. Xia, and J. Ivanov, “Multichannel seismic surface-wave methods for geotechnical applications,” *Proc. First Int. Conf. App …*, 2000.

[30] S. Foti, S. Parolai, D. Albarello, and M. Picozzi, “Application of Surface-Wave Methods for Seismic Site Characterization,” *Surv. Geophys.*, 2011.

[31] G. Das, “A Brief Review on Different Surface Wave Methods and Their Applicability for Non- Destructive Evaluation of Pavements,” *Nondestruct. Test. Eval.*, pp. 337–350, 2008.

[32] P. E. L.D. Olson and P. K. Miller, “Multiple Impact Surface Waves (MISW) – Improved Accuracy for Pavement System Thicknesses and Moduli vs. Spectral Analysis of Surface Waves (SASW),” in *ASCE GeoFlorida 2010 proceedings*, 2010, vol. 2, p. 210.

[33] K. Edip, M. Garevski, V. Sesov, and C. Butenweg, “Numerical simulation of wave propagation in soil media,” *Proc. 21st Eur. Young Geotech. Eng. Conf. Rotterdam*, pp. 140–145, 2011.

[34] A. Zerwer, G. Cascante, and J. Hutchinson, “Parameter Estimation in Finite Element Simulations of Rayleigh Waves,” *J. Geotech. Geoenvironmental Eng.*, 2002.

[35] R. L. Kuhlemeyer and J. Lysmer, “Finite element method accuracy for wave propagation problems,” *J. Soil Mech. Found. Div.*, 1973.

[36] C. T. Schröder and W. R. Scott, “A finite-difference model to study the elastic-wave interactions with buried land mines,” *IEEE Trans. Geosci. Remote Sens.*, vol. 38, no. 4 I, pp. 1505–1512, 2000.

[37] C. T. Schröder, “On the interaction of elastic waves with buried land mines: an investigation using the finite-difference time-domain method,” Georgia Institute of Technology, 2001.

[38] E.L.Wilson, “Static and Dynamic Analysis of Structures,” 2004.

[39] J.-Y. Shih, D. Thompson, and A. Zervos, “Assessment of Track-Ground Coupled Vibration Induced by High-Speed Trains,” *21st Int. Congr. Sound Vib.*, no. July, pp. 13–17, 2014.

[40] M. O. Al-Hunaidi, “Nondestructive evaluation of pavements using Spectral analysis of surface waves in the frequency wave-number domain,” *J. Nondestruct. Eval.*, vol. 15, no. 2, pp. 71–82, 1996.

[41] M. Iodice, J. Muggleton, and E. Rustighi, “The Detection of Vertical Cracks in Asphalt Using Seismic Surface Wave Methods,” *J. Phys. Conf. Ser.*, vol. 744, no. 1, 2016.

[42] N. Ryden, C. Park, P. Ulriksen, and R. Miller, “Branching of Dispersion Curves in Surface Wave Testing of Pavements,” 2009.

[43] C. B. Park, R. D. Miller, and J. Xia, “Multimodal Analysis of High Frequency Surface Waves,” 2009.

[44] T. Forbriger, “Inversion of shallow-seismic wavefields: I. Wavefield transformation,” *Geophys. J. Int.*, vol. 153, no. 3, pp. 719–734, 2003.

[45] S. Foti, R. Lancellotta, L. V. Socco, and L. Sambuelli, “Application of Fk Analysis of Surface for Geotechnical Characterization,” in *International Conferences on Recent Advances in Geotechnical Earthquake Engineering and Soil Dynamics*, 2001.

[46] A. Zerwer, “Near Surface Fracture Detection in Structural Elements Investigation Using Rayleigh Waves,” University of Waterloo, 1999.

[47] K. F. Graff, *Wave Motion in Elastic Solids*. 2012.

[48] M. Iodice, “Road and Soil Dynamic Characterization From Surface Measurements,” University of Southampton, 2017.

[49] N. Ryden and M. J. S. Lowe, “Guided wave propagation in three-layer pavement structures,” *J. Acoust. Soc. Am.*, 2004.

[50] R. Huggins, “A Report On Land Streamers: The Last Geophone You Will Ever Plant?,” *Near-Surface Views, Near-Surface Geophys. Sect. Soc. Explor. Geophys. 11, no. 1 (2004).*